



# Filamentary transport in high-power H-mode conditions and in no/small-ELM regimes to predict heat and particle loads on PFCs for future devices

---

presented by N. Vianello on behalf of MST I-Topic 21 scientific team

23 May 2018



This work has been carried out within the framework of the EUROfusion Consortium and has received funding from the Euratom research and training programme 2014-2018 under grant agreement No 633053. The views and opinions expressed herein do not necessarily reflect those of the European Commission.

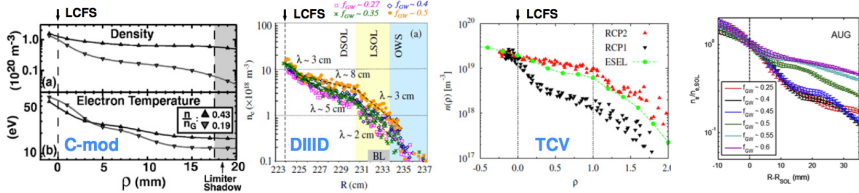


Volker Naulin, Matteo Agostini, Diogo Aguiam, Scott Allan, Matthias Bernert,  
Daniel Carralero Ortiz, Stefan Costea, Istvan Cziegler, Hugo De Oliveira, Joaquin  
Galdon-Quiroga, Gustavo Grenfell, Antti Hakola, Codrina Ionita-Schrittwieser,  
Heinz Isliker, Alexander Karpushov, Jernej Kovacic, Benoît Labit, Bruce Lipschultz,  
Roberto Maurizio, Ken McClements, Fulvio Militello, Jeppe Miki Busk Olsen, Jens  
Juul Rasmussen, Timo Ravensbergen, Bernd Sebastian Schneider, Roman  
Schrittwieser, Jakub Seidl, Monica Spolaore, Christian Theiler, Cedric Kar-Wai Tsui,  
Kevin Verhaegh, Jose Vicente, Nickolas Walkden, Zhang Wei, Elisabeth Wolfrum,  
W. Vijvers

# Background



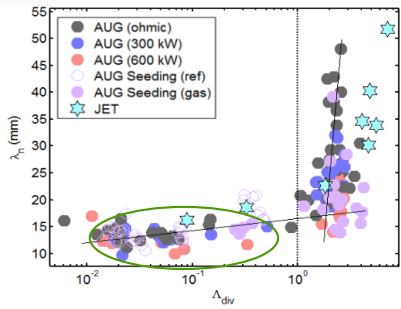
- ✓ Role of turbulence transport in the SOL density profile evolution is a well known feature (Carralero et al. 2014; Garcia et al. 2007; LaBombard et al. 2001; Rudakov et al. 2005).  
By increasing density, even without reaching detachment, SOL density profile tends to flatten



# Background



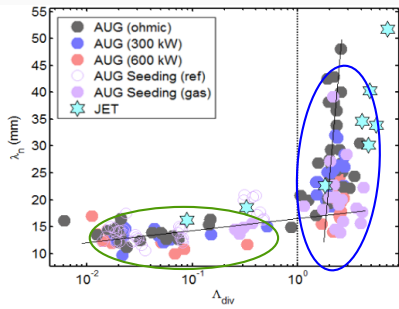
- ✓ AUG and JET (HT) (Carralero et al. 2015) suggest that  $\Lambda_{\text{div}} = \frac{L_{||}/c_s}{1/\nu_{ei}} \frac{\Omega_i}{\Omega_e}$  dominates this process through a transition from sheath-limited



# Background



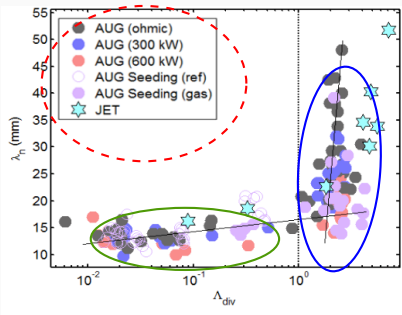
- ✓ AUG and JET (HT) (Carralero et al. 2015) suggest that  $\Lambda_{\text{div}} = \frac{L_{||}/c_s}{1/\nu_{ei}} \frac{\Omega_i}{\Omega_e}$  dominates this process through a transition from sheath-limited to inertial regime





# Background

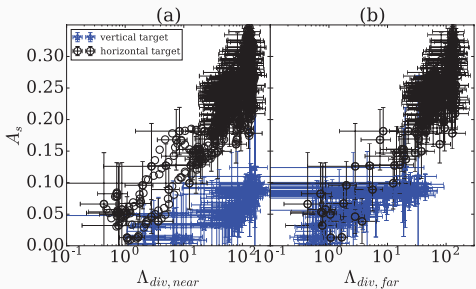
- ✓ AUG and JET (HT) (Carralero et al. 2015) suggest that  $\Lambda_{\text{div}} = \frac{L_{||}/c_s}{1/\nu_{ei}} \frac{\Omega_i}{\Omega_e}$  dominates this process through a transition from sheath-limited to inertial regime
- ✓ Tested by changing  $n_e$  and  $T_e$  through fueling/seeding/heating



# Background



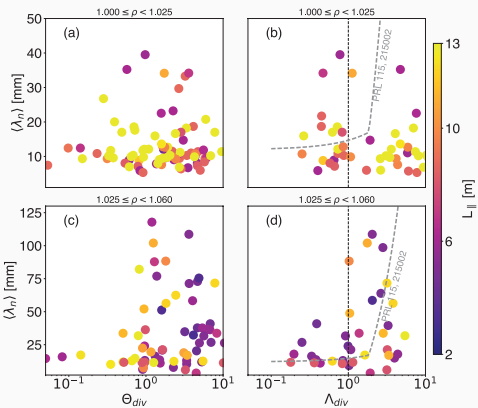
- ✓  $\Lambda_{div}$  does not describe properly evolution of upstream profile in JET-VT  
(Wynn et al. 2018)



# Background



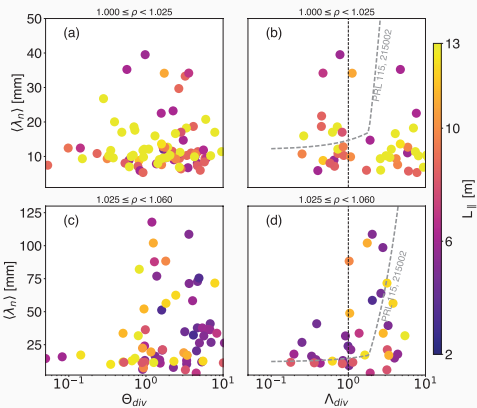
- ✓ On TCV (Vianello et al. 2017)  $\Lambda_{div}$  necessary but not sufficient to guarantee increase  $\lambda_n$  in the far SOL



# Background



- ✓ On TCV (Vianello et al. 2017)  $\Lambda_{div}$  necessary but not sufficient to guarantee increase  $\lambda_n$  in the far SOL
- ✓ Additional mechanisms suggested among which **effect of divertor neutrals (clogging mechanism)**



# Motivation and deliverables



- ✓ Relation between downstream divertor conditions and up-stream SOL profiles is not well understood. Influence of SOL blob structures on shoulder formation and divertor conditions is key element towards predictive capabilities. Joint effort within the EUROfusion framework to address this issue on all the MSTI devices (AUG, TCV and MAST-U)



- ✓ Relation between downstream divertor conditions and up-stream SOL profiles is not well understood. Influence of SOL blob structures on shoulder formation and divertor conditions is key element towards predictive capabilities. Joint effort within the EUROfusion framework to address this issue on all the MSTI devices (AUG, TCV and MAST-U)

A series of deliverables were foreseen by 2017 program

1. Cross-machine L-Mode shoulder dependence on current both at constant  $B_t$  and at constant  $q_{95}$ . Rationale: disentangle the effect of current and parallel connection length
2. Establish robust scenario for density shoulder profile in H-Mode and establish dependence on fuelling/neutral profiles/divertor condition
3. Fluctuations measurement on AUG to study filamentary transport under high-power H-Mode conditions and under different plasma configurations (SN, DN)
4. Study the role of ELM regimes, neutral compression and particle density in filamentary transport and related shoulder formation
5. Identify the contribution of collisionality and seeding on filamentary transport and related shoulder formation
6. Determine the effect of filaments and shoulder formation on target heat loads in different H-mode plasmas

# Motivation and deliverables

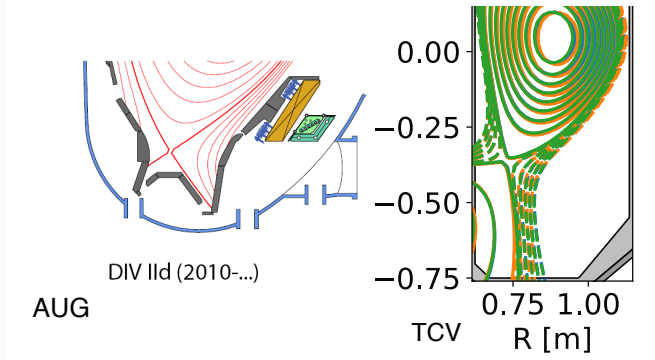


- ✓ Relation between downstream divertor conditions and up-stream SOL profiles is not well understood. Influence of SOL blob structures on shoulder formation and divertor conditions is key element towards predictive capabilities. Joint effort within the EUROfusion framework to address this issue on all the MSTI devices (AUG, TCV and MAST-U)

A series of deliverables were foreseen by 2017 program

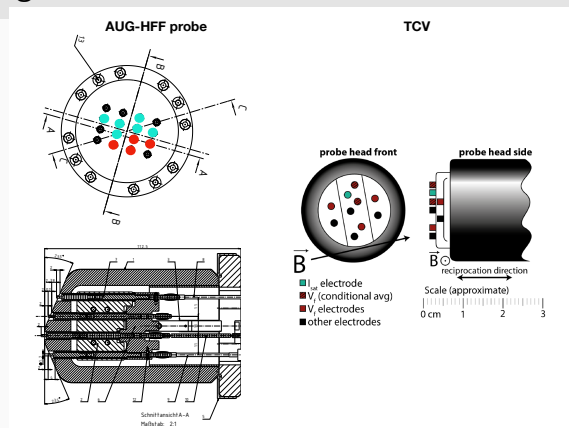
1. Cross-machine L-Mode shoulder dependence on current both at constant  $B_t$  and at constant  $q_{95}$ . Rationale: disentangle the effect of current and parallel connection length
2. Establish robust scenario for density shoulder profile in H-Mode and establish dependence on fuelling/neutral profiles/divertor condition
3. Fluctuations measurement on AUG to study filamentary transport under high-power H-Mode conditions and under different plasma configurations (SN, DN)
4. Study the role of ELM regimes, neutral compression and particle density in filamentary transport and related shoulder formation
5. Identify the contribution of collisionality and seeding on filamentary transport and related shoulder formation
6. Determine the effect of filaments and shoulder formation on target heat loads in different H-mode plasmas

Remember this is still a work in progress



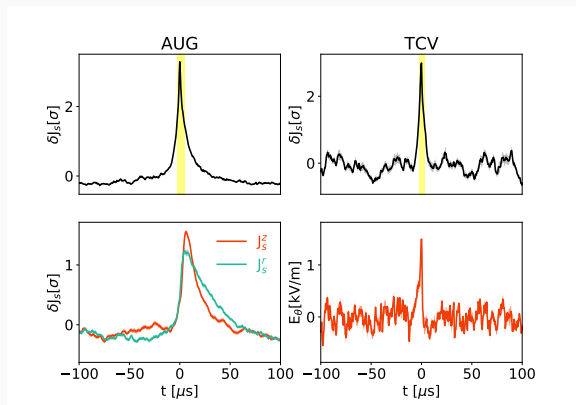
- ✓ **AUG:** Metallic wall, cryopumps, closed divertor with SP on vertical target, short divertor leg
- ✓ **TCV:** Carbon wall, completely open divertor; operated with relative long divertor leg, no cryopump

# Devices, diagnostics and methods



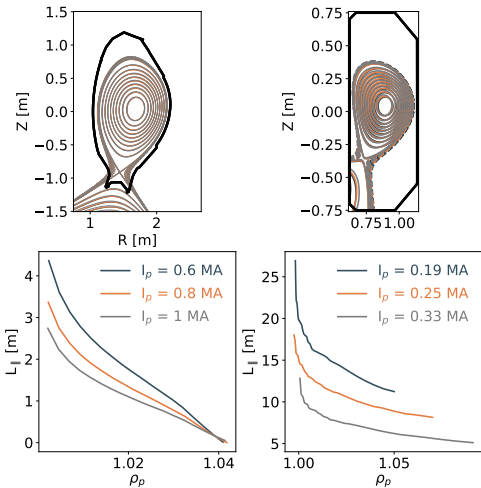
- ✓ **AUG:** Ion saturation current measured at different radial/poloidal position to get velocity from 2D cross-correlation
- ✓ **TCV:** A single  $j_{sat}$  measurement available, which implies different velocity estimate.  $v_r$  from  $\mathbf{E} \times \mathbf{B}$  evaluation from floating potentials  $v_z$  from 2D cross-correlation analysis (see Tsui, PoP submitted)

# Devices, diagnostics and methods



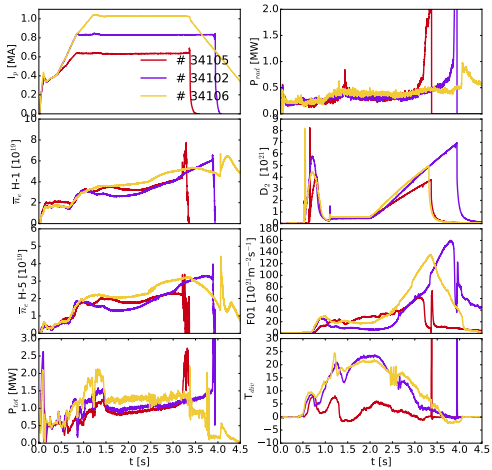
- ✓ Blob-size is  $\delta_b = \frac{\tau_b * v_{\perp}}{2}$
- ✓  $\tau_b$  estimated from FWHM of Conditional Average, binormal blob velocity estimated

# Current scan at constant $B_t$ in L-Mode plasma



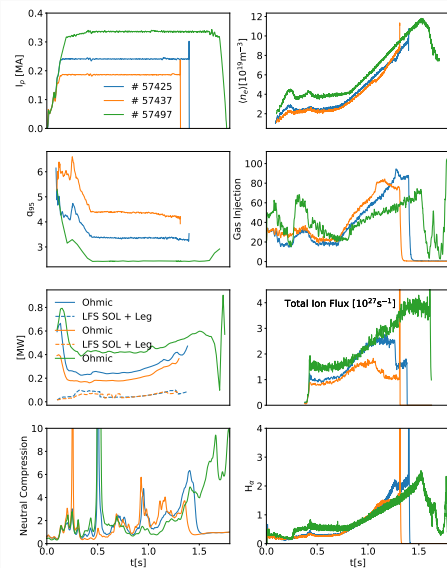
- ✓ Shape well matched in both the device
- ✓ The scan implies a modification of the  $L_{||}$  (shown from the X-point height to the outer target). Factor of 5 difference between the two machines

# Current scan at constant $B_t$ in L-Mode plasma



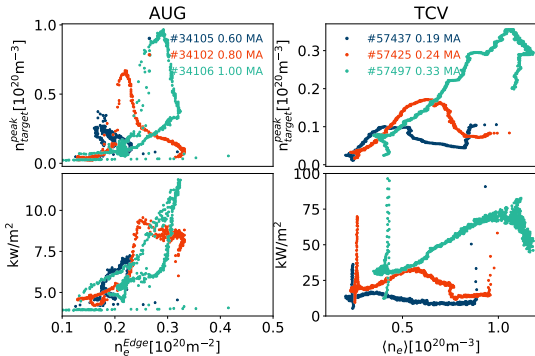
- ✓ AUG: Fueling reduced only at lower  $I_p$  to avoid earlier disruption. Comparable neutral pressure in the sub divertor region reached. 0.5 MW NBI additional power added to keep power in the SOL approximately constant

# Current scan at constant $B_t$ in L-Mode plasma



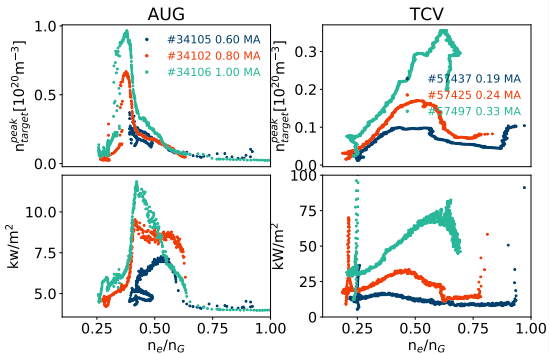
- ✓ TCV: Ohmic heating only. Similar neutral compression reached and  $D_\alpha$  radiation from the floor. Ion flux rollover reached in all the three current, although marginally at 330 kA

# Current scan at constant $B_t$ in L-Mode plasma



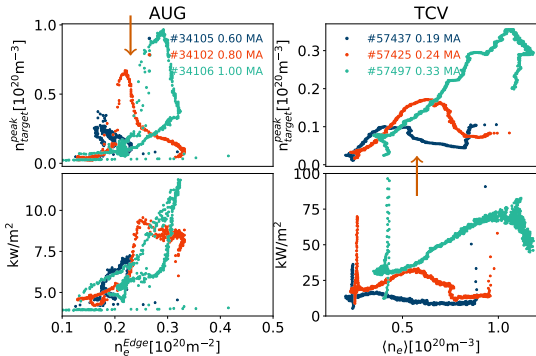
- ✓ In both the machines both the peak target density and the radiation close to divertor target exhibit rollover at increasing density with increasing current

# Current scan at constant $B_t$ in L-Mode plasma



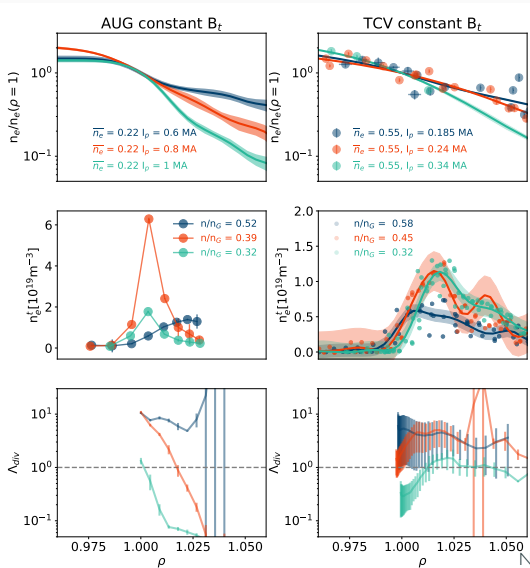
- ✓ Whenever considered as a function of Greenwald fraction the  $n_e^{\text{peak}}$  behaviors at different currents reconciled for both the machine AUG **partially for radiation movement**

# Current scan at constant $B_t$ in L-Mode plasma



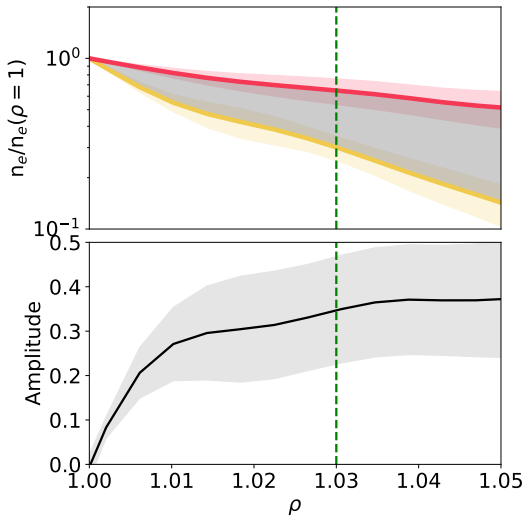
- ✓ We now consider the Target and upstream profiles at the same level of densities

# Current scan at constant $B_t$ in L-Mode plasma



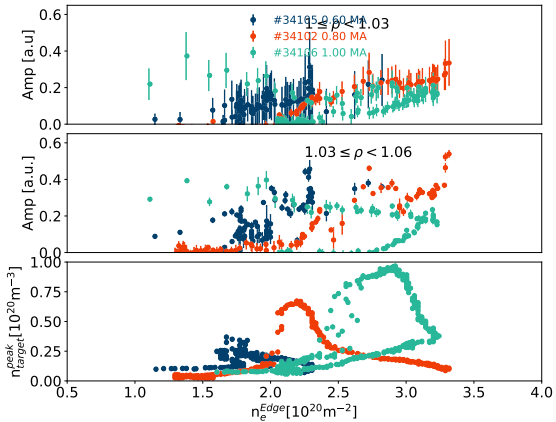
- ✓ We now consider the Target and upstream profiles at the same level of densities
- ✓ For both AUG and TCV flattening of normalized upstream profile reached **earlier in density at lower current**. For both the machine the increase of  $\lambda_n$  reached for larger values of  $\Lambda_{div}$

# Current scan at constant $B_t$ in L-Mode plasma



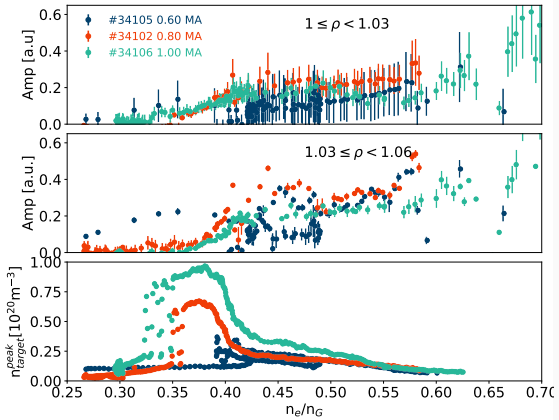
- ✓ Quantifying profile evolution using the **shoulder amplitude metric** introduce by Wynn and Lipschultz for JET (Wynn et al. 2018).
- ✓ Amplitude is the difference between normalized upstream density profiles
- ✓ Distinguishing behavior on the near and far SOL

# Current scan at constant $B_t$ in L-Mode plasma



- ✓ Amplitude evolve faster in density at lower current in the far SOL. Amplitude starts increasing close to the transition to highly-recycling regime as in JET HT (Wynn et al. 2018)

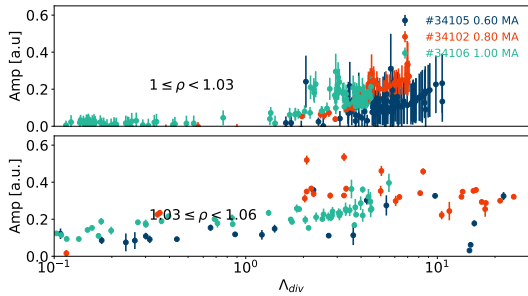
# Current scan at constant $B_t$ in L-Mode plasma



✓ Amplitude evolve faster in density at lower current in the far SOL. Amplitude starts increasing close to the transition to highly-recycling regime as in JET HT (Wynn et al. 2018) **but evolution is equivalent if considered vs greenwald fraction**

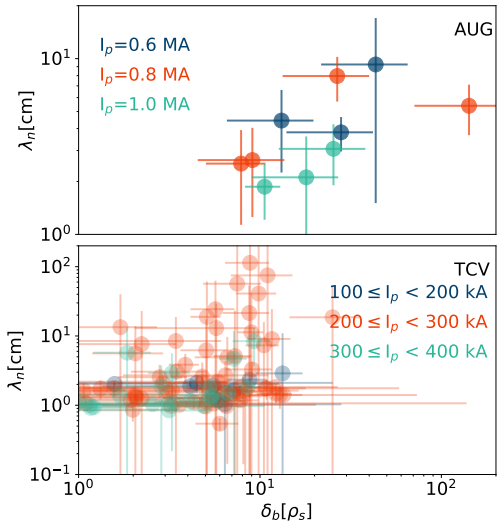
✓ Still some inconsistency at lower current in agreement with different detachment evolution

# Current scan at constant $B_t$ in L-Mode plasma



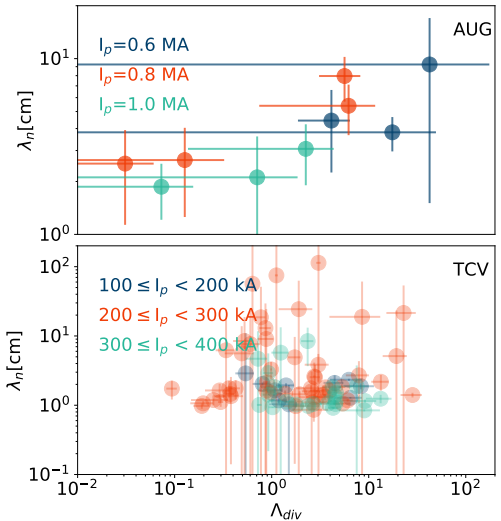
- ✓ Amplitude evolution reconciled in AUG if considered as a function of local evolution of  $\Lambda_{div}$

# Current scan at constant $B_t$ in L-Mode plasma



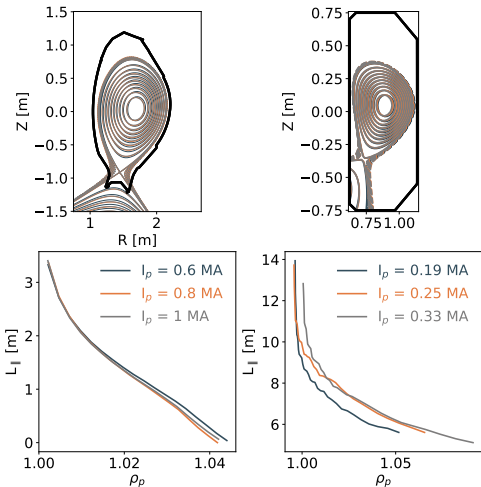
- ✓ For both AUG and TCV  $\lambda_n$  increases with blob size without significant difference within the current explored

# Current scan at constant $B_t$ in L-Mode plasma



✓ The evaluation of  $\lambda_n$  as a function of  $\Lambda_{\text{div}}$  confirms that this variable is insufficient to completely reconcile AUG and TCV

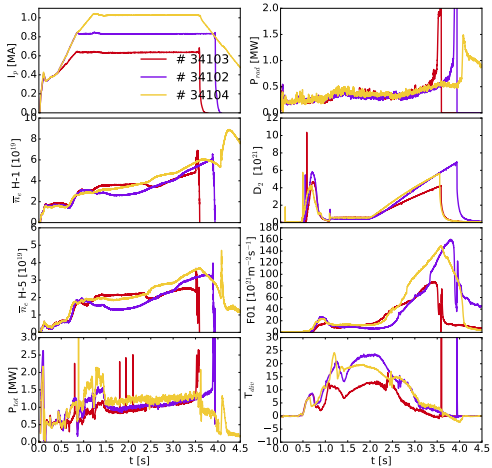
# Current scan at constant $q_{95}$



- ✓ Shape matched in within the single scan even though this required for TCV operation with very low toroidal field (0.8T)
- ✓ The parallel connection length remains almost unchanged

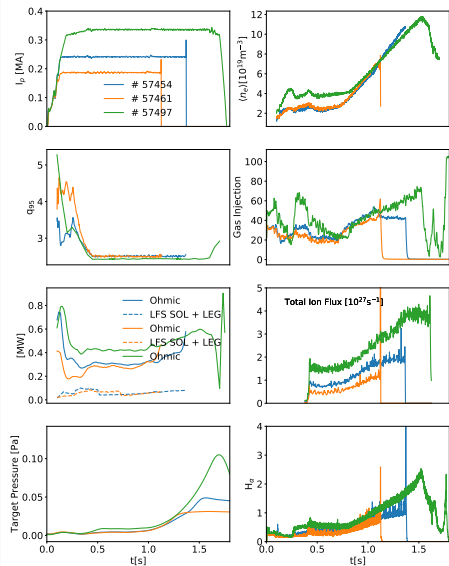


# Current scan at constant $q_{95}$



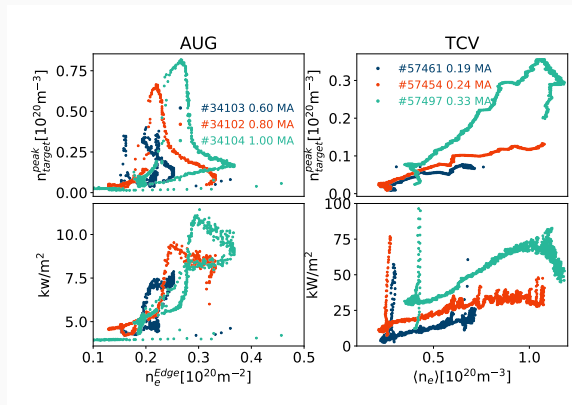
- ✓ AUG: As for the case of constant  $B_t$  we have pretty reproducible behavior matching basically the plasma condition in within the current scan

# Current scan at constant $q_{95}$



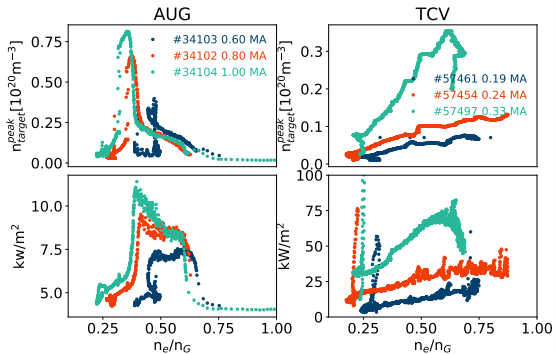
- ✓ TCV: Even at such an high density at lower current (and lower  $B_t$ ) no sign of target ion flux rollover/detachment

# Current scan at constant $q_{95}$



- ✓ AUG peak target density rollover occurs at lower density for lower current as well as radiation front movement. For TCV rollover achieved only at higher current: **lower  $I_p$**  does not exhibit sign of detachment even if high density is achieved. Consistent with lower volumetric recombination from DSS

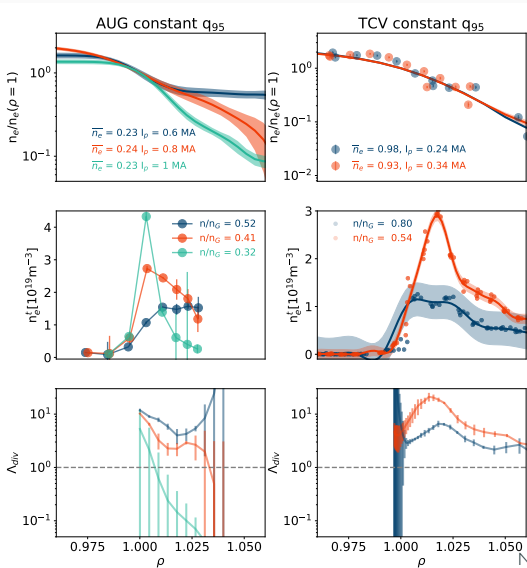
# Current scan at constant $q_{95}$



- ✓ Interestingly considering the behavior as a function of greenwald fraction does not reconcile the different current neither on AUG.



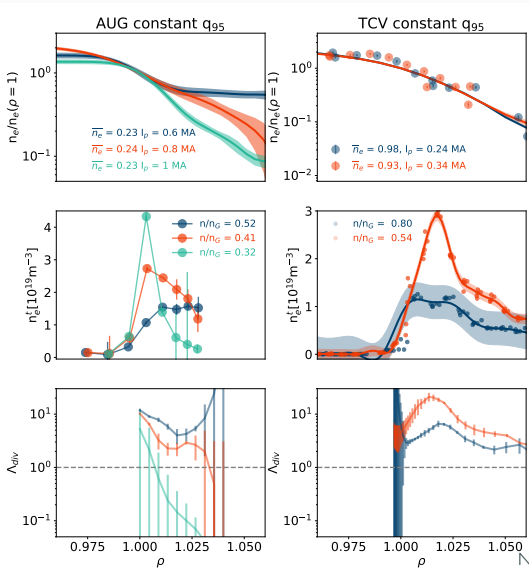
# Current scan at constant $q_{95}$



- ✓ For AUG upstream and target profiles still exhibit flattening earlier in density at lower current but **always at large values of  $\Lambda_{div}$** . For TCV no sign of upstream profile flattening **even at very large values of  $\Lambda_{div}$**

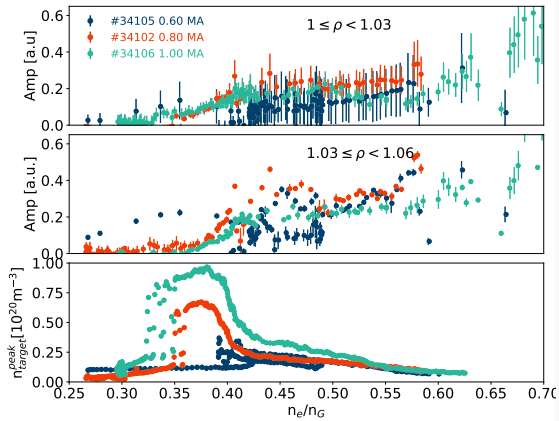


# Current scan at constant $q_{95}$



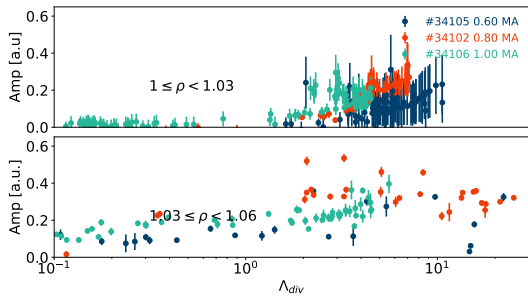
- ✓ For AUG upstream and target profiles still exhibit flattening earlier in density at lower current but **always at large values of  $\Lambda_{div}$** . For TCV no sign of upstream profile flattening **even at very large values of  $\Lambda_{div}$**
- ✓ This is due to the fact we did not reach divertor detachment which **seems mandatory for upstream profile modification**

# Current scan at constant $q_{95}$



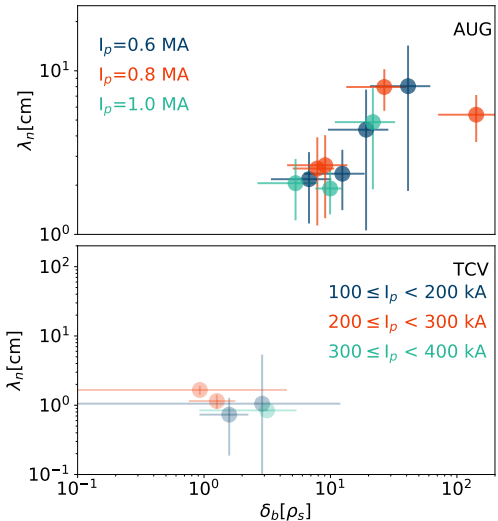
- ✓ AUG: Amplitude evolution as a function of greenwald fraction confirms that shoulder starts appearing at the onset of highly recycling regime

# Current scan at constant $q_{95}$



- ✓ AUG: Amplitude evolution as a function of  $\Lambda_{div}$  still reconcile the explored current scan

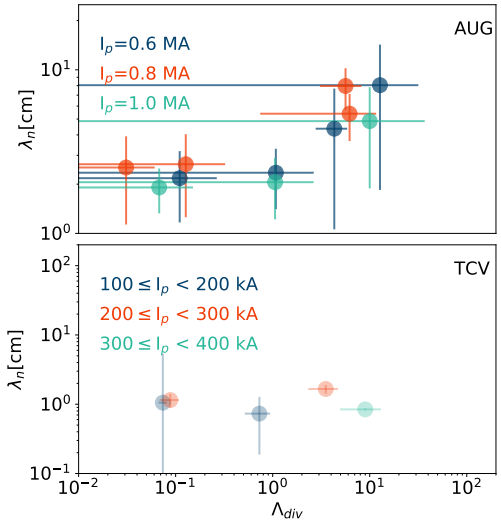
# Current scan at constant $q_{95}$



- ✓ AUG exhibit consistently an increase of  $\lambda_n$  with blob-size whereas for TCV the profile remains flat consistently with a small variation of  $\delta_b$



# Current scan at constant $q_{95}$

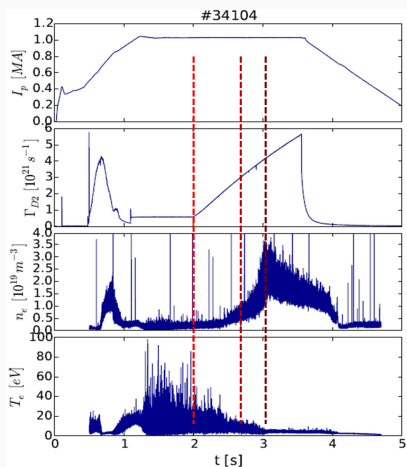


- ✓ And for TCV this is true even at high value of  $\Lambda_{div}$ .  $\Lambda_{div}$  is not sufficient to guarantee flat profiles on TCV.

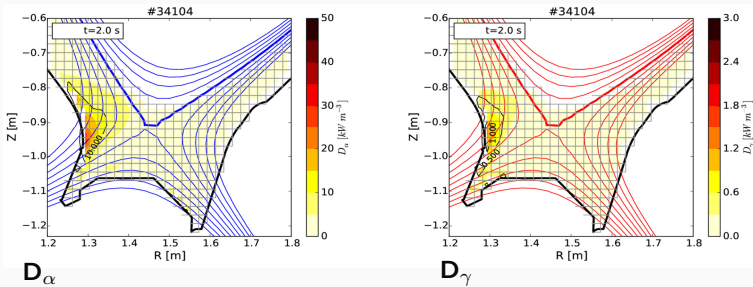
# Neutral behavior investigation on AUG



- ✓ Light emission analysis performed using 2 absolute calibrated CCD cameras with  $D_\alpha$  and  $D_\gamma$  filter
- ✓ Tomographic inversion using pixel technique assuming emission only outside the LCFS and neglecting reflection
- ✓ Inversion technique based on **S**imultaneous **A**lgebraic **R**econstruction **T**echnique (SART) with no input from equilibrium and no regularization
- ✓ Evolution during density ramp explored



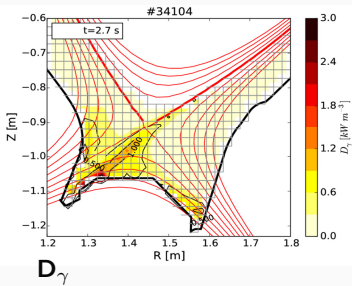
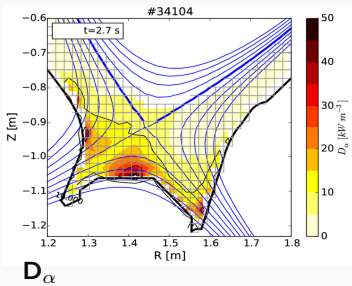
# Neutral behavior investigation on AUG



At the beginning of the fueling ramp emission localized in the HFS

(M. Agostini)

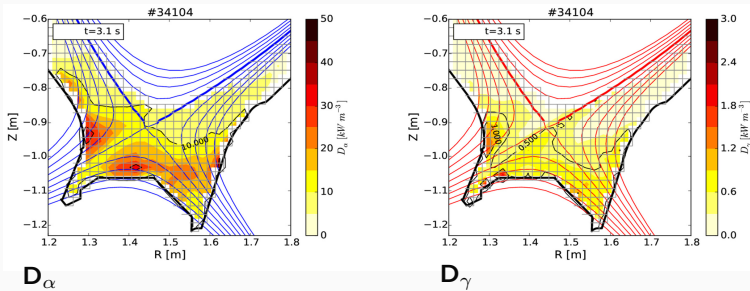
# Neutral behavior investigation on AUG



Radiation starts moving towards the X-point (different patterns  $D_\alpha$ ,  $D_\gamma$ )

(M. Agostini)

# Neutral behavior investigation on AUG



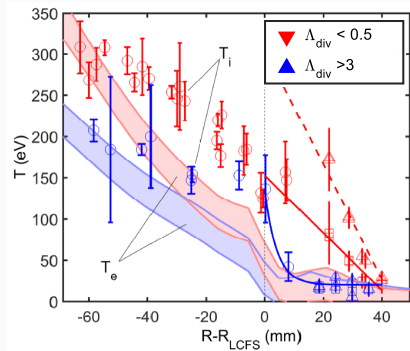
Emission propagate also towards the LFS and moves towards the CFR

(M. Agostini)

# Heat transport and power balance

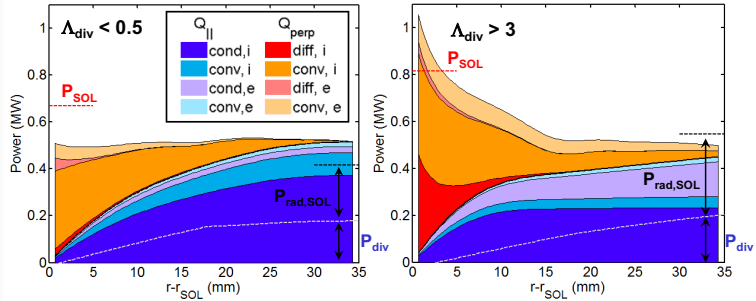


- ✓ Using a large database (around 30 discharges) in L-Mode detailed ion and electron temperature profiles collected
- ✓ Consistent ion temperature drop observed whenever shoulder is observed



(D. Carralero)

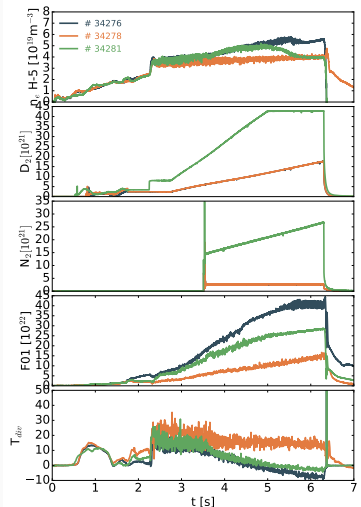
# Heat transport and power balance



- ✓ Parallel heat flux dominated by ion conduction whereas perpendicular component dominated by ion convection
- ✓ In high density regime a substantial fraction of  $P_{\text{SOL}}$  still remains in the  $Q_{\perp}$  for  $r - r_{\text{LCFS}} \sim 20$  cm

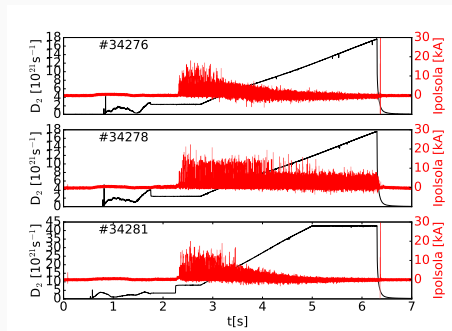
(D. Carralero)

# H-Mode analysis on AUG



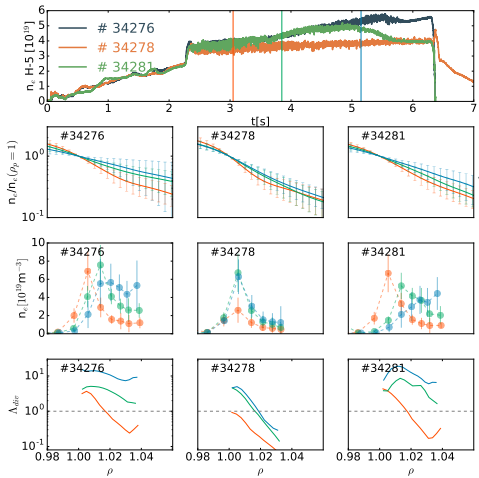
- ✓ We perform a series of shots in H-Mode with 6.5 total heating power where we changed the fueling and the efficiency of cryopumps. Specifically we have
  - ✓ # 34276 without the cryopumps
  - ✓ # 34278 with the same fueling as # 34276 but with the cryopump
  - ✓ #34281 where we increase fueling and seeding trying to mimic the same sub divertor pressure as # 34276
- ✓ Keeping the same fueling with the cryopump clearly reduce the pressure in the the sub-divertor area, we don't reach clear detachment and the edge density is constant even during the fueling ramp. Degraded H-mode reached later without the cryopump

# H-Mode analysis on AUG



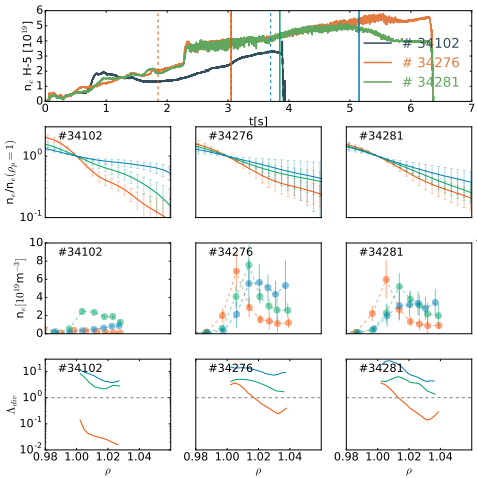
- ✓ Different behavior of ELM during the fueling ramp. ELM size and frequency changes strongly without the cryopump or during extreme fueling case

# H-Mode analysis on AUG



✓ The profiles for shot # 34278 with the cryopump and lower fueling remains more steep in all the three time windows and the plasma is still attached. Interestingly for shot # 34281 with the cryopumps and higher fueling the detachment is more pronounced

# H-Mode analysis on AUG

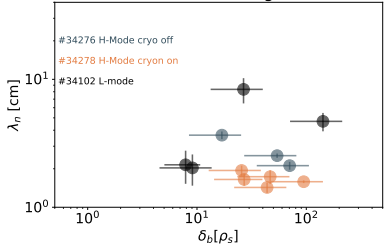


✓ The shoulder is almost comparable w.r.t. L-Mode plasma (even if higher density is needed)

# H-Mode analysis on AUG

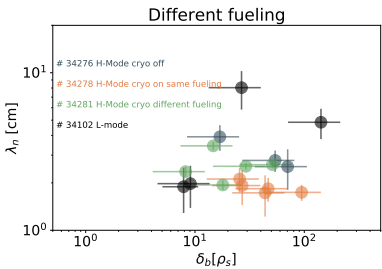


Same fueling



- ✓ Without the cryopumps, we reached flatter profiles with comparable inter-ELM resolved blob-size. This indicates strong neutral pressure effects in determining upstream profiles

# H-Mode analysis on AUG



- ✓ Increasing the fueling and correspondingly the divertor neutral pressure move towards a situation similar to # 34276 without the cryopump

# Conclusion



- ✓ Current scan at constant  $B_t$  and at constant  $q_{95}$  performed during density ramps L-Mode experiments both at AUG and TCV
- ✓ At constant  $B_t$  in both the experiments shoulder appears earlier in density at lower current: behavior reconciled if considered as a function of  $n_e/n_G$  and for AUG as a function of  $\Lambda_{div}$ . **Shoulder starts developing at the onset of highly recycling regime**
- ✓ Both the experiments exhibit at constant  $B_t$  flattening of the profile as blob size is increasing, independently from the current. The same behavior is observed during current scan at constant  $q_{95}$  **only on AUG**
- ✓ On TCV during the current scan at constant  $q_{95}$  detachment not reached and this **prevents upstream profile flattening**
- ✓ Evaluation of neutrals patterns in the divertor started on AUG.  $D_\alpha$  tomography reveal the movement of  $D_\alpha$  radiation towards the LFS CFR in analogy to JET HT
- ✓ Heat flux and power balance analysis in L-Mode plasmas on AUG. When shoulder appears a consistent fraction of perpendicular heat flux measured in the far SOL
- ✓ H-Mode experiments performed on AUG where fueling and pumping have been varied. **Proved inter-ELM profile flattening also in H-Mode but high neutral pressure (not only edge density) is needed**



A series of works are still on-going

- ✓ SOLPS modelling for both AUG and TCV for evaluation of collisionality along flux tube and power balance analysis
- ✓ HESEL (coupled to neutrals) for TCV current scan simulations for blob analysis
- ✓ Shoulder from Reflectometry analysis (**E. Seliunin**)
- ✓ Balmer series analysis for recombination analysis on TCV (**K. Verhaegh**) and MSI for radiation front neutrals
- ✓ GPI analysis and comparison with probe (**N. Walkden, I. Cziegler**)
- ✓ Particle acceleration associated to ELM filaments on AUG (**K. Mc Clements**)
- ✓ Neutral density estimate on divertor region on AUG (**M. Agostini**)